Low-temperature magnetization and spin-wave excitations in amorphous Ni-rich transition-metal—metalloid alloys

S. N. Kaul
Institut für Experimentalphysik IV, Ruhr Universität Bochum, 4630 Bochum, West Germany
(Received 16 March 1982)

Magnetization as a function of temperature has been measured for a number of amorphous Ni-rich transition-metal—metalloid alloys in the temperature range 4.2—300 K at various constant applied magnetic field values. These data when analyzed with caution not only yield reliable values for the coefficients B,C of the $T^{3/2},T^{5/2}$ terms appropriate for zero spin-wave energy gap and the mean-square range $\langle r^2\rangle$ of the exchange interaction but also give g values in agreement with those determined directly from the ferromagnetic resonance experiments. As a function of the Curie temperature T_C, the above parameters $(B,C,\langle r^2\rangle)$ are found to exhibit a systematic trend which is consistent with the predictions of a spin-wave theory based on the nearest-neighbor (NN) Heisenberg model. An empirical relation $D=D_0+mT_C$ is found to exist between the spin-wave stiffness coefficient, D, and T_C. While the collective-electron and NN Heisenberg models both fail to explain the finite positive value observed for D_0, the latter model gives the observed slope, m, value for $S=1$. Besides providing a theoretical justification for the observed relation between D and T_C, it has been shown that the Ruderman-Kittel-Kasuya-Yosida interaction plays a negligible role so far as the exchange mechanism leading to the present magnetization behavior is concerned. An estimate of the NN and next-nearest-neighbor (NNN) exchange coupling constants J_1 and J_2 reveals that J_2 is at least 1 order of magnitude smaller than J_1. Arguments are presented to show that the superexchange interactions brought into play by the presence of metalloid atoms and leading to an antiferromagnetic coupling between the spins localized on the NNN transition-metal atoms cannot be present in the amorphous alloys in question.

I. INTRODUCTION

Over the past few years, ample experimental evidence, based on inelastic neutron scattering,[1–5] low-temperature magnetization,[5–11] and Mössbauer[12–14] measurements, has been gathered to demonstrate that many amorphous ferromagnetic alloys exhibit well-defined long-wavelength spin-wave excitations which follow a normal ferromagnetic dispersion relation[15]

$$E(k)=\Delta+Dk^2+Ek^4+\cdots\ , \tag{1}$$

where $\Delta\ll Dk^2$ denotes an effective energy gap resulting from the dipole-dipole interactions[4,15] and that at low temperatures, magnetization, as in crystalline ferromagnets, follows the Heisenberg-model prediction

$$[M(0)-M(T)]/M(0)=\Delta M(T)/M(0)$$
$$=BT^{3/2}+CT^{5/2}+\cdots\ . \tag{2}$$

For a ferromagnet in the crystalline state, crystal momenta are quantized and the conventional spin-wave theory,[15] when applied to such a case, leads to the following relations between the coefficients B and C of the $T^{3/2}$ and $T^{5/2}$ terms in Eq. (2) and the spin-wave stiffness constant D:

$$B=\zeta(\tfrac{3}{2})[g\mu_B/M(0)](k_B/4\pi D)^{3/2} \tag{3}$$

and

$$C=\zeta(\tfrac{5}{2})[g\mu_B/M(0)](k_B/4\pi D)^{5/2}$$
$$\times(3\pi\langle r^2\rangle/4)\ , \tag{4}$$

where $\zeta(\frac{3}{2})=2.612$ and $\zeta(\frac{5}{2})=1.341$ are the Riemann ζ functions and $\langle r^2\rangle$ is the average mean-square range of the exchange interaction. Despite the fact that the translational invariance is completely absent in amorphous ferromagnets and the crystal momentum is no longer a good quantum number, Herring and Kittel,[16] from field-theoretical arguments, and Kaneyoshi,[17] from a viewpoint that amorphous magnets have a topological disordered structure of the type given by the random closed packing of atomic spheres, have shown that the spin-wave theory leading to Eqs. (1)—(4) is of more general validity than that suggested by the Heitler-

London-Heisenberg model from which it was originally derived. The major points in which the results reported to date on amorphous and crystalline ferromagnets differ and their implications have been recently summarized by Kaul[18] and by Ishikawa *et al.*[19]

An appraisal of the published low-temperature magnetization and neutron-diffraction data on some fcc and bcc crystalline ferromagnetic metals and alloys has revealed[20] a linear correlation between $T_C^{3/2}$ and $1/B$. From similar data reported on amorphous Co-P and $Fe_{75}P_{15}C_{10}$ alloys, it has been found[20] that such a direct proportionality between $1/B$ and $T_C^{3/2}$ still holds, but these data fall well below those for the crystalline ferromagnets. In view of Eq. (3), this observation implies that $D \propto T_C$. Recent magnetization measurements[9,11] on amorphous Fe-B-X (X=P,C,Si,Ge) and $Fe_{40}Ni_{40}B_{20-x}P_x$ alloys have indeed shown that such a linear relationship between D and T_C exists and that this linear dependence extrapolates to zero D for the former set of alloys at $T_C \simeq 380$ K and for the latter set at $T_C \simeq 200$ K. It should be noted that the above observations have been made from the data taken on alloys having T_C values higher than 450 K. These results are found to be inconsistent[11] with the predictions of a theory proposed by Katsuki and Wohlfarth[21] based on the itinerant electron model. However, it is still not clear whether this discrepancy between the experimental findings and the theoretical predictions is a result of an extrapolation from T_C values above 450 K or whether it is a genuine effect. In order to clarify this point, a systematic low-temperature magnetization study of particularly those amorphous alloys which have low T_C values is needed. Keeping this aim in mind, we chose to conduct this type of study on nickel-rich transition-metal–metalloid amorphous alloys which do possess low T_C values.

II. EXPERIMENTAL PROCEDURE AND DATA ANALYSIS

Amorphous alloy ribbons used in the present work were prepared by the rapid-quenching technique and had cross sections varying from 0.02×1.0 mm^2 to 0.05×2.5 mm^2. The glassy alloys known commercially as Metglas® 2826, 2826 A, and 2826 B were procured from the Allied Chemical Corporation, New Jersey, whereas the remaining samples were obtained from the General Electric Company, New York. With the use of the Faraday method, magnetization of several 10-mm ribbon lengths (stacked in the sample holder) was measured as a function of temperature from 4.2 to 300 K at various constant applied field values in the range from 3 to 15 kOe. In order to minimize the demagnetizing field effects, the magnetic field was applied in the plane of the ribbon pieces parallel to their length. A typical heating or cooling rate of 0.5 K/min and a small positive pressure of the helium exchange gas in the sample chamber were maintained to ensure a good thermal contact between the sample and the resistance thermometers. Details concerning the Faraday apparatus and the temperature measurement can be found in our previous reports.[22,23] The data taken on samples chosen from the different parts of the same alloy ribbon in the "as-received" condition are found to be reproducible to within 1%.

In determining the coefficients B and C appearing in Eq. (2) from the magnetic measurements performed in presence of an applied field H, the effective field

$$H_{\text{eff}} = H - 4\pi N M(0) + H_A$$

(where N is the demagnetizing factor and H_A the anisotropy field), which contributes to the energy gap in the spin-wave spectrum, must be taken into account by using a modified version of Eq. (2) given by[15,24]

$$\Delta M(T)/M(0) = B_{3/2} F(\tfrac{3}{2}, t_H) t^{3/2} + C_{5/2} F(\tfrac{5}{2}, t_H) t^{5/2} \cdots , \quad (5)$$

where

$$B_{3/2} = B T_C^{3/2}, \quad C_{5/2} = C T_C^{5/2}, \quad t = T/T_C ,$$

$$t_H = T_g/T = g\mu_B H_{\text{eff}}/k_B T ,$$

and

$$F(s, t_H) = [\zeta(s)]^{-1} \sum_{n=1}^{\infty} n^{-s} \exp(-n t_H) .$$

Since $t_H \ll 1$ in the present temperature range, the Robinson expansion of the functions $F(\frac{3}{2}, t_H)$ and $F(\frac{5}{2}, t_H)$ given by[25]

$$F(\tfrac{3}{2}, t_H) \approx [\zeta(\tfrac{3}{2})]^{-1} [\zeta(\tfrac{3}{2}) - 3.54 t_H^{1/2} + 1.46 t_H - 0.104 t_H^2 + \cdots] \quad (6)$$

and

$$F(\tfrac{5}{2}, t_H) \approx [\zeta(\tfrac{5}{2})]^{-1} [\zeta(\tfrac{5}{2}) - 2.61 t_H + 2.36 t_H^{3/2} - 0.730 t_H^2 + \cdots] \quad (7)$$

was used while fitting the data on various samples to Eq. (5). At first, a least-squares fit of the data to the spin-wave terms alone [Eq. (5)] was made over the range 0–4 K of gap temperatures with B and C allowed to vary independently. It was immediately noticed that a very broad minimum in the standard deviation σ vs T_g plot results, and corresponding to

TABLE I. Density, magnetic, and spin-wave parameters, and mean-square range of the exchange interaction for the present amorphous alloys and crystalline Fe and Ni. Numbers in the parentheses denote estimated uncertainty in the least significant figure. Sample numbers are as follows: 1, $Fe_{10}Ni_{70}B_{19}Si_1$; 2, $Fe_{13}Ni_{67}B_{19}Si_1$; 3, $Fe_{16}Ni_{64}B_{19}Si_1$; 4, $Fe_{20}Ni_{60}B_{19}P_1$; 5, $Fe_{20}Ni_{60}B_{20}$; 6, $Fe_{20}Ni_{60}P_{14}B_6$; 7, $Fe_{29}Ni_{49}P_{14}B_6Si_2$, 8, $Fe_{30}Ni_{50}P_{14}B_6$; 9, $Fe_{32}Ni_{36}Cr_{14}P_{12}B_6$; 10, $Fe_{40}Ni_{40}P_{14}B_6$; 11, Fe (Cryst.); 12, Ni (Cryst.).

Sample no.	ρ (g/c.c.)	g	$M(0)$ (G)	T_C (K)	$(T/T_C)_{max}$	B (10^{-6} $K^{-3/2}$)	$B_{3/2}$	C (10^{-8} $K^{-5/2}$)	$C_{5/2}$	D (meV Å^2)	D/T_C (meV Å^2 K^{-1})	$\langle r^2 \rangle$ (Å^2)
1	8.04[a]	2.07(3)	345.2	186.5(15)	0.80	212(8)	0.54(2)	23.2(70)	0.110(33)	53(2)	0.28(1)	7.0(26)
2	8.00[a]	2.07(3)	414.6	268.5(15)	0.80	127(5)	0.56(2)	9.7(38)	0.115(45)	66(2)	0.25(1)	6.1(30)
3	7.97[a]	2.07(3)	483.9	338(2)	0.76	84(3)	0.52(2)	5.3(23)	0.112(48)	78(2)	0.23(1)	5.9(31)
4	7.94[a]	2.06(2)	598.4	406(2)	0.72	59(2)	0.48(2)	3.5(11)	0.117(37)	86(4)	0.21(1)	6.1(27)
				410[b]						80[b]	0.20[b]	
5	7.94[c]	2.06(2)	583.6	419(2)	0.65	57(3)	0.49(2)	3.2(8)	0.115(30)	90(4)	0.21(1)	6.1(22)
6	7.73[d]	2.07(3)	428.6	228(2)	0.80	154(6)	0.53(2)	13.9(56)	0.109(44)	57(2)	0.25(1)	6.2(30)
7	7.51[e]	2.07(2)	525.7	375(2)	0.75	70(3)	0.51(2)	3.7(14)	0.100(40)	84(3)	0.22(1)	5.4(26)
				377[f]		65(3)[f]	0.48(3)[f]	1.5(5)[f]	0.040(20)[f]			
		2.09[g]		380[g]	0.80[g]	59(4)[g]	0.44(3)[g]	1.0(3)[g]	0.030(10)[g]			
8	7.63[d]	2.06(2)	620.7	430(2)	0.67	56(3)	0.50(3)	2.6(11)	0.101(40)	87(3)	0.20(1)	4.9(27)
9	7.46[e]	2.07(2)	447.6	250(1)	0.80	137(5)	0.54(2)	11.6(5)	0.115(45)	60(3)	0.24(1)	6.1(32)
10	7.52[d]	2.05(2)	754.0	520(1)	0.58	38(2)	0.45(2)	1.4(5)	0.090(30)	99(3)	0.19(1)	4.5(20)
		2.05(2)[h]		537[f]	0.58[f]	38(2)[f]	0.47(3)[f]	1.2(5)[f]	0.080(30)[f]			
				528[b]						100[b]	0.19[b]	
11[i]		2.09	1752.0	1043	0.13	3.4(2)	0.115(7)	0.1(1)	0.040(40)	286(11)	0.27(1)	10.1(123)
12[i]		2.19	508.0	631	0.19	7.5(2)	0.119(3)	1.5(2)	0.150(20)	397(7)	0.63(1)	95.7(177)

[a]From the density value measured in Ref. 46 for the amorphous $Fe_{20}Ni_{60}B_{20}$ alloy, we calculate the packing fraction using the Goldschmidt atomic radii for twelve-fold coordination in the case of transition-metal atoms and the tetrahedral covalent radii for the metalloids, i.e., 1.27 Å for Fe, 1.24 Å for Ni, 1.17 Å for Si, 1.10 Å for P, and 0.88 Å for B. The packing fraction so obtained has the value 0.697 which was then used to calculate the density of the alloys of other nearby compositions, thereby normalizing them to the measured value.

[b]J. J. Rhyne, J. W. Lynn, F. E. Luborsky, and J. L. Walter, J. Appl. Phys. 50, 1583 (1979); room-temperature value.

[c]Reference 46.

[d]J. J. Becker, F. E. Luborsky, and J. L. Walter, IEEE Trans. Magn. 13, 988 (1977).

[e]F. E. Luborsky, in *Ferromagnetic Materials,* Ref. 43, p. 451.

[f]Reference 12.

[g]Reference 10.

[h]Reference 26.

[i]Reference 24.

this broad minimum the range of the acceptable values of B and C is also very wide. In order to arrive at reliable values for these coefficients and to narrow down the range of acceptable values, the internal consistency conditions that the coefficients B and C are independent of temperature and applied field and that T_g varies with H_{eff} according to

$$T_g=(g\mu_B/k_B)H_{\text{eff}} \tag{8}$$

were imposed (note that the applied field H has been corrected only for the demagnetizing field and not for the anisotropy field H_A since a rough esimate of H_A shows that $H_A \ll H$). The values for the coefficients B and C for the present alloys obtained by this fitting procedure, originally adopted by Argyle *et al.*[24] for evaluating the values for these coefficients for crystalline ferromagnets, are given in Table I.

With a view to test the validity of Eq. (8), the coefficient C for each sample was kept constant at its value given in Table I and both T_g and B were allowed to vary. It is observed that consistent with Eq. (8) the positions of the minima in σ vs T_g curves move progressively to higher values of T_g as H is increased. The T_g values corresponding to these minima, when plotted against H_{eff}, yield a straight line which passes through origin for each of the alloys investigated. To illustrate this behavior, a T_g vs H_{eff} plot for Metglas® 2826 is shown in Fig. 2(a). The values for g calculated from the slope of such straight lines and included in Table I are found to be in excellent agreement (see Table I) with those determined for the same or similar amorphous alloys from the ferromagnetic resonance experiments.[10,26]

Realizing that besides the spin-wave excitations there exist Stoner single-particle excitations which also contribute to the low-temperature magnetization of a ferromagnet, the next step of the data analysis was to include in Eq. (5) an additional term AT^2 which denotes the single-particle contribution. Based on the observation that the low-temperature magnetization data fit reasonably well to a fictitious T^n term with n between 1.6 and 1.7 depending on the applied field strength, it can be easily concluded that the single-particle excitations do not give a dominant contribution to the magnetization in the presently studied amorphous alloys. That the exponent n is noticeably greater than 1.5 originates partly from the energy gap and partly from the field dependence of n and can be accounted for[27] by using $BF(\frac{3}{2},t_H)$ in place of B as the coefficient of the $T^{3/2}$ term. To ascertain whether or not the AT^2 replaces $CT^{5/2}$ in the role of a second dominant term, C was held constant at its previously determined value (given in Table I), and T_g was set equal to the theoretical value calculated from Eq. (8) for each of the four chosen field values 3, 5, 10, and 15 kOe, whereas A and B were allowed to vary in order to fit the data over three temperature ranges (different for different samples): starting from 4.2 K and extending up to $0.9T_C$ and 300 K for alloys having T_C values below and above 300 K, respectively. The resulting values of both A and B were found to be very much temperature dependent. The temperature dependence of B was about 4 times larger than that observed previously when A was set equal to zero and B and C were allowed to vary. These results indicate that the contribution arising from single-particle excitations, if significant, is much smaller than even the $CT^{5/2}$ term.

III. RESULTS AND DISCUSSION

In Fig. 1(a) the typical low-temperature magnetization behavior of the present amorphous ferromagnetic alloys is exemplified by plotting for a few of them the relative deviation of magnetization from its value at 0 K (no distinction between the values of magnetization at 4.2 and 0 K has been made in the present work), i.e., $\Delta M(T)/M(0)$ against the reduced temperature (T/T_C) at a constant applied field value of ~ 10 kOe. The solid curves through the data points represent the temperature dependence of magnetization predicted by Eq. (5) with the choice of the coefficients B and C given in Table I. This table gives, besides the magnetic and spin-wave parameters, the values for the average mean-square (ms) range $\langle r^2\rangle$ of the exchange interaction calculated using the presently determined values of B, C, and D in the relation

$$\langle r^2\rangle=[\zeta(\tfrac{3}{2})/\zeta(\tfrac{5}{2})](16/3k_B)(C/B)D\ . \tag{9}$$

With decreasing T_C, different parameters, whose values are summarized in Table I, present the following trend: (i) The upper temperature limit $(T/T_C)_{\max}$, up to which the spin-wave contribution to magnetization [Eq. (5)] alone accounts for the observed low-temperature magnetization behavior, shifts to higher temperatures. This is basically a manifestation of the fact that the temperature range over which the $T^{3/2}$ law dominates becomes wider and wider as T_C decreases. (ii) The calculated average ms range of the exchange interaction and D/T_C (which again is an approximate measure of the range of exchange interaction) both show a slow increase. This observation is further elucidated by the plots of $\langle r^2\rangle$ vs T_C and D/T_C vs T_C in Fig. 1(b). Despite such an increase in $\langle r^2\rangle$ with lowering T_C, the value of the rms range for the alloy with the lowest T_C value barely exceeds the typical mean nearest-neighbor transition-metal—transition-metal distance[28] of 2.55 Å in such amorphous ferromagnets.

However, due to the large uncertainty limits for $\langle r^2 \rangle$, the only conclusion that can be drawn with confidence is that the exchange interaction in amorphous ferromagnetic alloys is short ranged and can at best involve the next-nearest neighbors, whereas its range in crystalline ferromagnets greatly exceeds even the next-nearest-neighbor distance. (iii) The normalized coefficient $C_{5/2}$ remains apparently constant at a value which compares favorably with the corresponding values observed for crystalline Fe and Ni, whereas the reduced coefficient $B_{3/2}$ increases at a very slow rate (which progressively decreases with decreasing T_C) until a value $T_C \cong 300$ K is reached below which it becomes independent of T_C, and for the present alloys possesses values that are roughly *4 times larger* in magnitude than those found in crystalline ferromagnets. Similar deductions[5,10,12,13,18] have been made in the past from a comparison be-

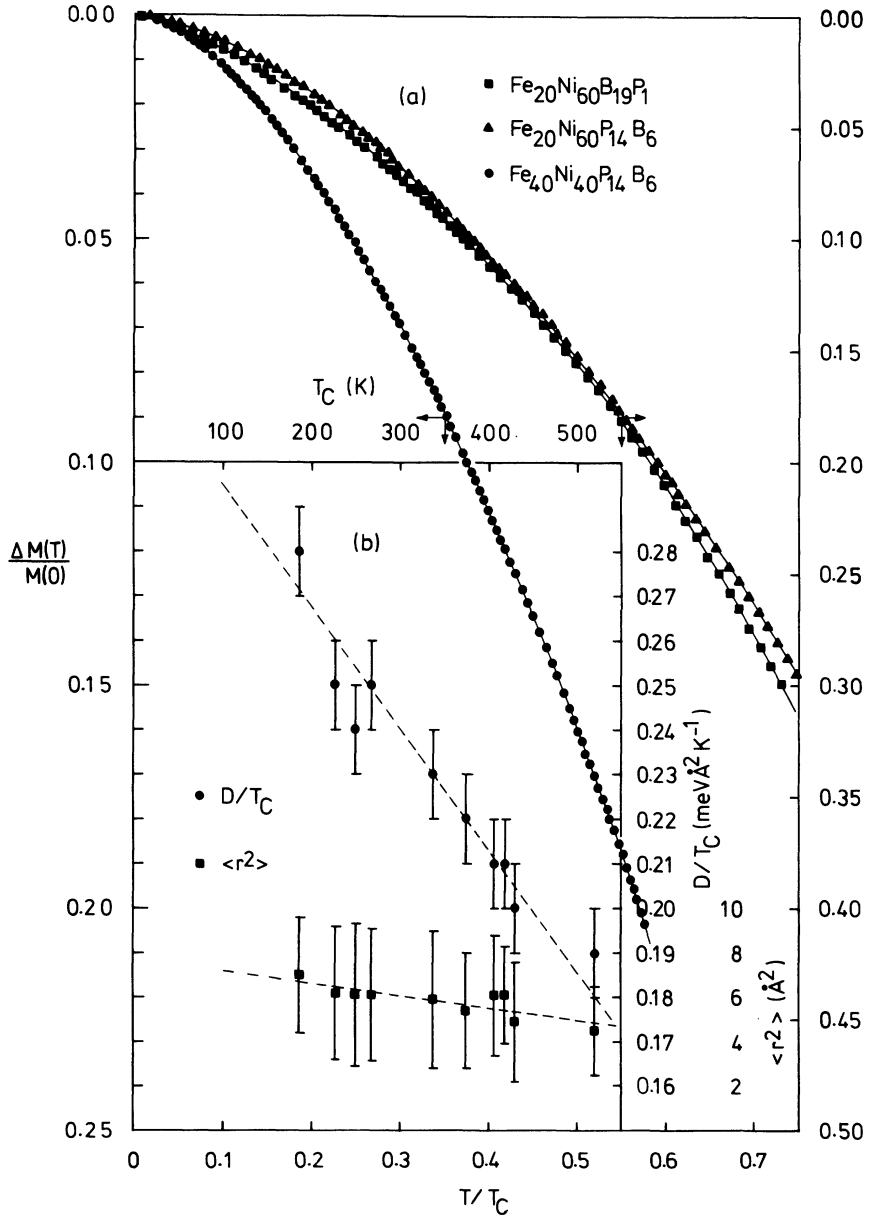

FIG. 1. (a) Fractional decrease in magnetization with temperature above 4.2 K ($\Delta M=0$ at $T=4.2$ K) for amorphous $Fe_{20}Ni_{60}B_{19}P_1$, $Fe_{20}Ni_{60}P_{14}B_6$, and $Fe_0Ni_{40}P_{14}B_6$ (Metglas® 2826) alloys in presence of an applied magnetic field value of 10, 11 and 10 kOe, respectively. The solid curves through the data points are the theoretical variations predicted by Eq. (5) of the text with the choice of the coefficients $B_{3/2}$ and $C_{5/2}$ given in Table I. (b) D/T_C vs T_C and $\langle r^2 \rangle$ vs T_C plots. The dashed lines through the data points represent the least-squares fit to the data.

tween the values of $B_{3/2}$ and $C_{5/2}$ observed in crystalline and amorphous ferromagnets.

Consistent with the above-mentioned variation of $B_{3/2}$ with T_C, a plot of $1/B$ vs $T_C^{3/2}$ shown in Fig. 2(b) demonstrates that $1/B \propto T_C^{3/2}$ [dashed line in Fig. 2(b)] only for $T_C \lesssim 300$ K; the data points deviate more and more from this straight line as T_C increases beyond ~ 300 K. In view of Eq. (3), the nonlinearity observed in the $1/B$ vs $T_C^{3/2}$ plot at high T_C implies that no direct correlation should exist between D and T_C particularly in the high T_C region, but when the data shown in Fig. 2(b) are converted into a D vs T_C plot using Eq. (3), a linear curve results for the entire range of T_C values (see Fig. 3). It will be shown later that this apparent inconsistency arises from the fact that $D \neq 0$ at $T_C = 0$ and $M(0)$ is *not constant* for the alloys in question.

Returning to Fig. 3, it is found that the data can be represented very well by the empirical relation[29]

$$D = D_0 + mT_C \,, \tag{10}$$

where D_0 and m are, respectively, the intercept on the ordinate and the slope of the straight-line curve. In this figure, results of the recent magnetization measurements[5,30] on amorphous $(Fe_{1-x}Ni_x)_{75}P_{16}B_6Al_3$ and $(Fe_{1-x}Ni_x)_{77}Si_{10}B_{13}$ alloys have also been included. These data are seen to pass smoothly with the trend exhibited by the present data. A least-squares fit to the complete

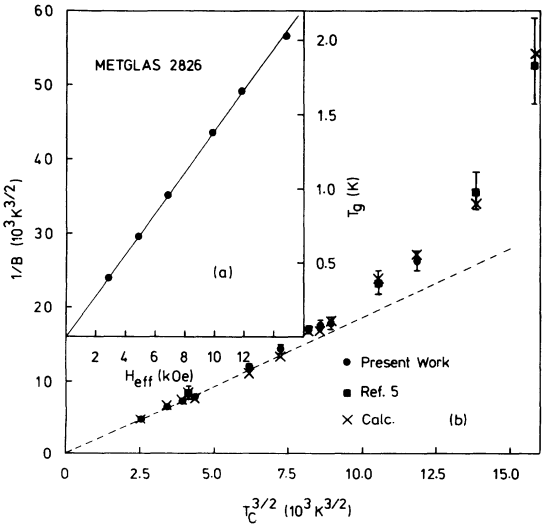

FIG. 2. (a) Spin-wave energy gap temperature T_g plotted against the effective magnetic field H_{eff} for Metglas® 2826. The solid line through the data points is the least-squares fit to the data and the slope of this straight line gives the value for g. (b) $1/B$ vs $T_C^{3/2}$ plot for the amorphous alloys used in this work. Results of Ref. 5 (filled squares) and $1/B$ values calculated using Eq. (17) of the text (crosses) are also included for comparison.

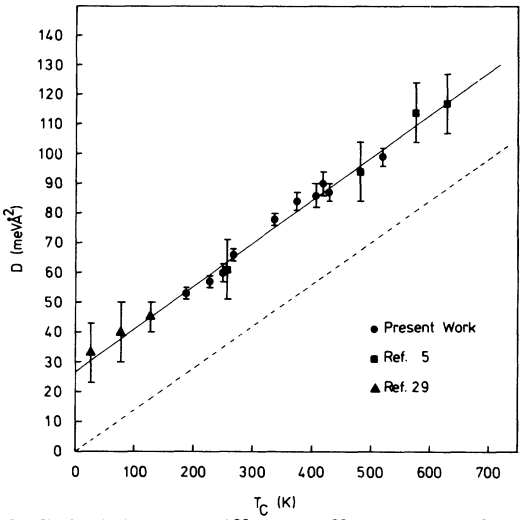

FIG. 3. Spin-wave stiffness coefficient D as a function of the Curie temperature T_C for the present amorphous alloys; the results obtained on the other Ni-rich transition-metal—metalloid alloys in Refs. 5 and 29 are also included in this figure. The solid line through the data points is the result of a least-squares fit to the complete data shown in this figure. The dashed line denotes the theoretical variation predicted by a nearest-neighbor Heisenberg model for $S=1$.

data shown in Fig. 3 based on Eq. (10) yields $D_0 = 27 \pm 2$ meV Å^2 and $m = 0.144 \pm 0.020$ meV Å^2 K^{-1}. The error limits in these quantities have been determined from the least-squares fits through the upper and lower uncertainty limits of the data points. A linear relation between D and T_C of the type given by Eq. (10) has also been observed[30,31] previously for amorphous $(Fe_{1-x}Ni_x)_{77}Si_{10}B_{13}$ and $(Co_{1-x}Ni_x)_{75}P_{16}B_6Al_3$ alloys with the values for $D_0(m)$ as 29 meV Å^2 (0.125 meV Å^2 K^{-1}) and 12 meV Å^2 (0.100 meV Å^2 K^{-1}), respectively.

Before we proceed to discuss the above results within the framework of the collective-electron and Heisenberg models, both of which predict a linear correlation between D and T_C, it should be mentioned that the customary approach[11,30] of also including the D values directly measured by the inelastic neutron scattering technique in such a figure has not been followed in the present work because of the following reason. Recent inelastic neutron-diffraction studies[32] on amorphous $(Fe_{1-x}Ni_x)_{75}P_{16}B_6Al_3$ alloys in the concentration range $0.6 \leq x \leq 0.83$ (these alloys exhibit at high temperatures a transition to long-range ferromagnetism which at low temperatures gives way to a spin-glass behavior) have resolved the discrepancy between the D values deduced from the magnetization measurements, D_M, and those values measured directly by

the inelastic neutron-diffraction technique, D_N, observed earlier[5] for the alloys with x in the vicinity of 0.7 by revealing that for the alloys just mentioned D increases as usual with decreasing temperature up to a certain temperature below which the spin-glass state sets in and D begins to decrease with decreasing temperature. Therefore, a meaningful comparison between D_M and D_N is possible only when the inelastic neutron scattering study is performed over an extended temperature range rather than at a single temperature (in most cases the room temperature), as is usually the case. The former type of studies are available to date only on a few Fe-rich (Fe,Ni)-metalloid amorphous alloys and their results do indeed fall on the curve shown in Fig. 3.

With the assumption that the Curie temperature T_C is determined by the Stoner single-particle excitations alone, Katsuki and Wohlfarth,[21] based on the collective-electron model, have derived for weak itinerant ferromagnets the following relation between D and T_C:

$$D = k_B T_C a^2 f(n) , \tag{11}$$

where a is the nearest-neighbor distance and $f(n)$ is a function of the number of electrons per atom determined by the band structure. Equation (11) reduces to a simple analytical form only when the effective-mass approximation is used. In this approximation

$$D = [\pi k_B / 6(2)^{1/2} k_F^2] T_C , \tag{12}$$

where k_F is the Fermi radius. Besides predicting that $D=0$ at $T_C=0$, Eq. (12) gives a value for the slope as 0.014 meV Å^2 K^{-1} when the typical value of $k_F=1.5$ Å^{-1} is used. It is immediately noticed that this theory cannot account for the finite value observed for D_0 and yields a slope value which is at least 1 order of magnitude smaller than that observed presently. In order to overcome the main disadvantage of the effective-mass approximation, that it concerns an open band, these authors have extended the previous calculations to a simple cubic metal with the result that beyond a certain critical value of I_{eff}/W (I_{eff} and W are the effective interaction between the magnetic carriers and the bandwidth, respectively), D as a function of T_C exhibits the following behavior. Starting from $D=0$ at $T_C=0$, D initially increases at a constant rate, goes through a maximum and then decreases at a nonlinear rate to zero, again, but this time at a finite value of T_C. Both the zeros of D correspond to a ferromagnetic instability (for details, see Ref. 21). Contrary to the above prediction, the recent investigations[30,32] have shown that in amorphous (Fe,Ni)-metalloid alloys the ferromagnetic instability occurs at a finite value of D. Although Katsuki,[33] while refining the earlier theory by taking into account both Stoner single-particle and spin-wave excitations, showed later that the theoretical D vs T_C curve given in Ref. 21 gets modified so much so that it resembles the observed curve for fcc Fe-Ni and Ni-Cu alloys and that its initial part qualitatively represents the trend found in bcc Fe-Cr alloys, this modified theory, as its previous version, serves as an illustrative guide only and is severely limited so far as the interpretation of a finite value of D_0 is concerned.

The results are next discussed in the light of the Heisenberg model. For a nearest-neighbor cubic ferromagnet, the Heisenberg model gives the spin-wave energy as[15,34]

$$E(k) = Dk^2 \tag{13a}$$

with

$$D = SzJa^2/3 , \tag{13b}$$

where J is the exchange coupling constant between the nearest-neighbor pairs, S is the localized atomic spin, a is the nearest-neighbor distance, and z is the number of the nearest neighbors. If the expression for T_C obtained in the molecular-field approximation,[15] i.e.,

$$T_C = [2S(S+1)/3k_B] zJ \tag{14}$$

is used to eliminate zJ in Eq. (13b), it is possible to relate D and T_C as follows:

$$D = [k_B a^2 / 2(S+1)] T_C . \tag{15}$$

Equation (15) evidently shows that a D vs T_C plot should be a straight line which passes through the origin. Thus, the nearest-neighbor Heisenberg model also cannot provide an explanation for the intercept D_0 observed in Fig. 3. We will return to this point below. The next step is to see if this model can correctly predict the observed slope. Using $a=2.55$ Å, Eq. (15) gives the slope, $m=D/T_C$, values of 0.140 and 0.187 meV Å^2 K^{-1} for $S=1$ and $S=\frac{1}{2}$, respectively. The former slope value is in excellent agreement with that determined experimentally. A firm support to the argument that this agreement between the observed and predicted slope value is *not* just a *coincidence* is provided by the theoretical calculations[35] based on the nearest-neighbor Heisenberg model. These calculations give the numerical value for the normalized coefficient $B_{3/2}$ in Eq. (5) as 0.587 for $S=\frac{1}{2}$ and 0.512 for $S=1$. A glance at Table I reveals that the experimental values agree strikingly well with those estimated from a nearest-neighbor Heisenberg model; the present values being closer to the theoretical value for $S=1$ than that for $S=\frac{1}{2}$. Such an agree-

ment between the theoretical and experimental values looks more convincing when the above Heisenberg values are compared with those observed for crystalline Fe and Ni (see Table I).

Thomson and Thompson[36] have recently shown that the $T^{3/2}$ behavior of the low-temperature heat capacity, magnetization, and resistivity observed in crystalline CuMn, AgMn, AuMn, and PdMn spin-glasses can be understood in terms of a simple spin-wave model in which the neighboring spins are correlated through the Ruderman-Kittel-Kasuya-Yosida (RKKY) interactions. Now that the spin-glass behavior has also been observed in the amorphous transition-metal–metalloid alloys on the nickel-rich side,[30,37–39] it is logical to think that the RKKY interaction may give an important contribution to the low-temperature magnetization behavior for the present alloys too. Starting from a Hamiltonian which involves, in addition to the direct nearest-neighbor Heisenberg exchange, the indirect exchange interaction of the RKKY form, we show in Appendix A that the introduction of the RKKY interaction leads to a finite value of D_0 but contrary to the present observations this value is not only negative but also negligibly small. From this result, we conclude that the RKKY interaction has a negligible role to play so far as the exchange mechanism leading to the observed magnetization behavior of the present alloys is concerned.

Other possible forms of exchange interaction that are also expected to result in a finite value of D_0 could be either the Heisenberg interaction which extends beyond the nearest-neighbor distance or the superexchange interaction between the next-nearest-neighbor magnetic atoms mediated by a metalloid atom separating them, or both. In Appendix B, we treat the general case where the nearest-neighbor and the next-nearest-neighbor spin pairs interact through an exchange interaction of the Heisenberg form with the corresponding exchange coupling constants denoted by J_1 and J_2, respectively, and arrive at the same relation between D and T_C as Eq. (10) with the following expressions for the slope, m and the intercept D_0:

$$m = k_B a_1^2/2(S+1) \tag{16a}$$

and

$$D_0 = z_2 J_2 (a_2^2 - a_1^2) S/3 , \tag{16b}$$

where a_1 and a_2 are the nearest-neighbor and the next-nearest-neighbor distances, and z_2 is the number of the next-nearest neighbors. While Eq. (16a) gives the observed slope value for $S=1$ and $a_1=2.55$ Å, Eq. (16b) can be used to estimate the value of J_2. Taking $a_1=2.55$ Å, $a_2=4.35$ Å (corresponding to the first and second peaks in the radial distribution function[28]), $z_2 \cong 6$, $S=1$, and $D_0=27$ meV Å^2 (the observed value), the value for J_2 comes out to be ~ 1.1 meV.

Theoretical attempts[40–43] to fit a wide variety of experimental data taken on Fe,Co,Ni yield the values for the nearest-neighbor exchange coupling constant J_1 in the range 10–50 meV. Similar efforts to estimate the value of J_1 in amorphous ferromagnetic alloys are relatively few in number. From our earlier magnetization study[44] on amorphous $(Ni_{1-x}Fe_x)_{80}B_{20}$ and $(Ni_{1-x}Fe_x)_{80}P_{14}B_6$ alloys, we find that the values of J_1 deduced using the relation

$$\langle J \rangle = (1-x)^2 J_{\text{Ni-Ni}} + 2x(1-x) J_{\text{Fe-Ni}} + x^2 J_{\text{Fe-Fe}}$$

also fall within the above-mentioned range. A comparison between the estimated values of J_1 and J_2 reveals that J_2 in such amorphous systems is at least 1 order of magnitude smaller than J_1. Assuming the functional dependence of the exchange integral J on distance r of the form

$$J(r) = J_1 \exp\{\alpha[(r/a_1)-1]\}$$

with $J(r)=0$ for $r \geq 1.25 a_1$, Krey,[35] within the framework of the Heisenberg model, has shown that with increasing $|\alpha|$ for negative values of α, T_C decreases, the normalized coefficient $B_{3/2}$ shows a weak increasing trend while the reduced coefficient $C_{5/2}$ remains practically constant, and the temperature range over which the $(T/T_C)^{3/2}$ term dominates becomes wider whereas for positive values of α, these parameters exhibit the opposite trend. Our observations (i) and (iii) conform very well with the theoretical variations predicted for T_C, $B_{3/2}$, $C_{5/2}$, and $(T/T_C)_{\max}$ by Krey's theory[35] for negative values of α. Again, such an agreement between the theory and experiment is consistent with the finding that the estimated values for J_1 and J_2, when used in the above expression for $J(r)$, yield the values of α in the range from -3.3 to -5.5. Considering the fact that $J_2 \ll J_1$, it is not surprising to find that a nearest-neighbor Heisenberg model gives a fairly good description of the low-temperature magnetic behavior of amorphous ferromagnets.

Although the extended Heisenberg model is capable of giving a plausible interpretation for the parameters (m, D_0) in the empirical expression, Eq. (10), it does not provide a straightforward explanation for the observation that for crystalline ferromagnets, where the exchange is presumably as long ranged as in the amorphous counterparts, $D_0 \cong 0$. In the text below, we suggest that this inconsistency can be removed in case that superexchange interactions that favor a parallel alignment of the next-nearest-neighbor spin pairs exist in amorphous ferromagnetic alloys containing metal-

loid atoms.

Superexchange interactions brought into play by the presence of metalloid atoms in these amorphous materials are expected[45] to lead to an antiferromagnetic coupling between the moments of the next-nearest-neighbor transition-metal atoms, and their strength can be comparable in magnitude to that of the direct Heisenberg exchange between the nearest neighbors. In view of Eq. (16b), the superexchange interactions of this type should result in an *anomalously large negative* value of D_0. This prediction directly contradicts the observed behavior, and hence we conclude that such interactions cannot be present in the alloys in question. However, we cannot rule out the existence of the superexchange interactions that favor a parallel alignment of the spins localized on the next-nearest-neighbor sites and give a major contribution to the next-nearest-neighbor exchange interaction J_2 that we observe. If such interactions exist, it is easy to understand as to why $D_0 \cong 0$ only for crystalline ferromagnets and not for the amorphous ferromagnetic alloys.

Finally, we return to the apparent paradox that in spite of a nonlinear relation between $1/B$ and $T_C^{3/2}$ [Fig. 2(b)], a direct correlation exists between D and T_C (Fig. 3). With a view to resolve this apparent discrepancy between the plots depicted in Figs. 2(b) and 3, Eqs. (3) and (10) are combined to yield the relation

$$1/B = [M(0)/g\mu_B \zeta(\tfrac{3}{2})](4\pi m/k_B)^{3/2} T_C^{3/2} \times [1+(D_0/mT_C)]^{3/2} . \quad (17)$$

If T_C is allowed to vary while keeping all other parameters [including $M(0)$] that appear in the above relation constant, Eq. (17) predicts that $(1/B) \propto T_C^{3/2}$ only when $D_0 = 0$, whereas a nonlinear relation between $1/B$ and $T_C^{3/2}$ should exist when D_0 is finite. So it is *not obvious* from Eq. (17) as to how one can reconcile to the present situation ($D_0 \neq 0$) where a relation $(1/B) \propto T_C^{3/2}$ [dashed line in Fig. 2(b)] holding at low T_C is no longer valid at high T_C (where $1/B$ increases at a much faster rate than that suggested by the $T_C^{3/2}$ power law) *unless* one realizes that there is a *strong correlation* between $M(0)$, which *differs widely* from one amorphous alloy to the other, and $[1+(D_0/mT_C)]^{3/2}$. This is easily verified as follows: The values $D_0 = 27$ meV Å^2, $m = 0.144$ meV Å^2 K^{-1}, and those of $M(0)$, g, and T_C given in Table I and Ref. 5 for different amorphous ferromagnetic alloys when used in Eq. (17) lead to the $1/B$ values, denoted in Fig. 2(b) by crosses, which are found to reproduce remarkably well the observed functional dependence of $1/B$ on T_C [see Fig. 2(b)].

IV. SUMMARY AND CONCLUSIONS

The results of magnetization measurements performed on amorphous Ni-rich transition-metal—metalloid alloys from 4.2 to 300 K at various constant applied magnetic field values in the range from 3 to 15 kOe when analyzed with caution yield reliable values for the magnetic and spin-wave parameters which, in turn, are found to exhibit a systematic trend as a function of the Curie temperature T_C. This trend conforms very well with that predicted by a spin-wave theory based on the nearest-neighbor (NN) Heisenberg model. Of particular interest among the observed relations between various parameters and T_C is the direct correlation $D = D_0 + mT_C$ observed between the spin-wave stiffness coefficient D and T_C. This relation has been discussed in terms of the theories based on the collective-electron and the NN Heisenberg models. While both the models utterly fail to explain the finite value observed for D_0, the latter model gives the correct slope value m for $S = 1$.

In order to arrive at the exchange mechanism responsible for a finite value of D_0, we have considered two cases within the framework of the Heisenberg model: (i) when both the RKKY and direct NN exchange interactions are simultaneously present and (ii) when the direct exchange interaction involves not only the nearest neighbors but also the next-nearest neighbors. We have then calculated the modified spin-wave dispersion relations with the result that a negative but negligible value for D_0 is obtained in the former case whereas in the latter case a positive finite D_0 value results if the nature of exchange interaction is such that it favors a parallel alignment of spins localized on the next-nearest-neighbor (NNN) sites. The value for the slope m predicted by a NN Heisenberg model is shown to remain unaffected when in addition to the direct NN exchange, either the RKKY or the NNN exchange interaction is also included. With the use of the typical values for different parameters appearing in the theoretical expression obtained for D_0 in the second case [Eq. (16b)], the NNN exchange coupling constant is found to be at least 1 order of magnitude smaller than the NN exchange coupling constant. This finding is consistent with the fact that a spin-wave theory based on the NN Heisenberg model gives a fairly good description of the low-temperature magnetic behavior of the present amorphous alloys. Arguments are put forward to show that the superexchange interactions leading to an antiferromagnetic coupling between the moments on the NNN transition-metal atoms cannot exist in the alloys in question. In addition, Stoner single-particle excitations have been shown to give a negligible contribution to the temperature dependence of

magnetization in these alloys.

Finally, the measured variation of the spin-wave energy gap with the applied field strength permits the determination of g values which are found to be in excellent agreement with their corresponding values obtained from the ferromagnetic resonance experiments on the same or similar amorphous ferromagnetic alloys.

ACKNOWLEDGMENTS

The author wishes to thank Professor M. Rosenberg for providing some of the samples used in the present work, Professor S. Methfessel for his keen interest in this work, and Dr. P. K. Shukla for helpful discussions.

APPENDIX A

The Hamiltonian of interest is the sum of contributions arising from (i) H_z, the interaction of the localized spin with the external magnetic field directed along the z axis, the quantization direction; (ii) H_{dd}, the direct exchange interaction between localized spins; and (iii) H_{sd}, the indirect exchange interaction between localized moments brought about by conduction electrons, usually referred to as the RKKY interaction:

$$H = H_z + H_{dd} + H_{sd} , \tag{A1}$$

where

$$H_z = -g\mu_B H_0 \sum_i S_{iz} ,$$

$$H_{dd} = -\sum_i \sum_{j\neq i} J_{ij} \vec{S}_i \cdot \vec{S}_j ,$$

and

$$H_{sd} = -\sum_n \sum_{n\neq m} J_0 F(2k_F R_{mn}) \vec{S}_m \cdot \vec{S}_n ,$$

with

$$J_0 = -(9\pi/2) A Z^2 ,$$

$$A = [\,|J_{sd}(0)|^2/E_F\,] ,$$

and

$$F(x) = (x\cos x - \sin x)/x^4 .$$

Here Z is the valency and $R_{mn} = |\vec{R}_{mn}| = |\vec{R}_m - \vec{R}_n|$ while the remaining symbols have their usual meaning. If we now restrict the direct exchange to the nearest neighbors only and denote the exchange coupling between the spin localized on the site i and its z nearest neighbors at positions $\vec{\delta}$ relative to i by J, the exchange interaction H_{dd} becomes

$$H_{dd} = -J \sum_i \sum_{\vec{\delta}} \vec{S}_i \cdot \vec{S}_{i+\vec{\delta}}$$

$$= -J \sum_i \sum_{\vec{\delta}} [(S_i^+ S_{i+\vec{\delta}}^- + S_i^- S_{i+\vec{\delta}}^+)/2 + S_{iz} S_{(i+\vec{\delta})z}] .$$

Transforming[47] the operators S^+, S^-, and S_z to $b_{\vec{k}}^\dagger$ (magnon-creation) and $b_{\vec{k}}$ (magnon-annihilation) operators and neglecting for the low-lying excitations the fourth- and higher-order terms in magnon operators, the various contributions to the Hamiltonian H reduce to[47]

$$H_z = -g\mu_B H_0 NS + g\mu_B H_0 \sum_{\vec{k}} b_{\vec{k}}^\dagger b_{\vec{k}} \tag{A2}$$

(N being the number of localized sites in the total volume V). We have

$$H_{dd} = -J \sum_i \sum_{\vec{\delta}} \left[SN^{-1} \sum_{\vec{k}\vec{k}'} e^{-i(\vec{k}-\vec{k}')\cdot\vec{R}_i} e^{i\vec{k}'\cdot\vec{\delta}} b_{\vec{k}} b_{\vec{k}'}^\dagger + SN^{-1} \sum_{\vec{k}\vec{k}'} e^{i(\vec{k}-\vec{k}')\cdot\vec{R}_i} e^{-i\vec{k}'\cdot\vec{\delta}} b_{\vec{k}}^\dagger b_{\vec{k}'} \right.$$
$$\left. + \left[S - N^{-1} \sum_{\vec{k}\vec{k}'} e^{i(\vec{k}-\vec{k}')\cdot\vec{R}_i} b_{\vec{k}}^\dagger b_{\vec{k}'} \right] \left[S - N^{-1} \sum_{\vec{k}\vec{k}'} e^{i(\vec{k}-\vec{k}')\cdot\vec{R}_i} e^{i(\vec{k}-\vec{k}')\cdot\vec{\delta}} b_{\vec{k}}^\dagger b_{\vec{k}'} \right] \right] .$$

Using the relations $\sum_i e^{i(\vec{k}-\vec{k}')\cdot\vec{R}_i} = N\Delta(\vec{k}-\vec{k}')$ and $[b_{\vec{k}}, b_{\vec{k}'}^\dagger] = \delta_{\vec{k}\vec{k}'}$, defining $\gamma_{\vec{k}} = z^{-1} \sum_{\vec{\delta}} e^{i\vec{k}\cdot\vec{\delta}} = \gamma_{-\vec{k}}$, and noting that $\sum_{\vec{k}} \gamma_{\vec{k}} = 0$, the above expression simplifies into

$$H_{dd} = -NzJS^2 + 2zJS \sum_{\vec{k}} (1-\gamma_{\vec{k}}) b_{\vec{k}}^\dagger b_{\vec{k}} . \tag{A3}$$

In the long-wavelength limit, i.e., $|\vec{k}\cdot\vec{\delta}| \ll 1$, $\gamma_{\vec{k}} \simeq 1 - (a_0 k)^2/z$ for cubic lattices of lattice constant a_0, and Eq. (A3) takes the form

$$H_{dd} = -NzJS^2 + 2JS \sum_{\vec{k}} (a_0 k)^2 b_{\vec{k}}^\dagger b_{\vec{k}} . \tag{A4}$$

In case we neglect the boundary effects so that the spatial sums can be carried out independently, i.e.,

$$\sum_{\vec{R}_n}\sum_{\vec{R}_m}\rightarrow\sum_{\vec{R}_n}\sum_{\vec{r}=\vec{R}_m-\vec{R}_n},$$

and adopt the same procedure as above, H_{sd} finally reduces to

$$H_{sd}=-J_0NS^2\sum_{\vec{r}}F(2k_Fr)-J_0S\sum_{\vec{k}}\left[\sum_{\vec{r}}F(2k_Fr)e^{i\vec{k}\cdot\vec{r}}+2\left[\sum_{\vec{r}}F(2k_Fr)e^{i\vec{k}\cdot\vec{r}}-\sum_{\vec{r}}F(2k_Fr)\right]b^{\dagger}_{\vec{k}}b_{\vec{k}}\right]. \tag{A5}$$

Breaking the sum over $\vec{r}$ into a *sum* within a sphere of radius b plus an *integral* over the rest of the sample and realizing that for the magnon wavelength $\lambda\gg b$, the *sum* for a *cubic* crystal is zero and the sums over $\vec{r}$ appearing in Eq. (A5), in the limit $b\rightarrow 0$, simplify as follows:

$$\sum_{\vec{r}}F(2k_Fr)=4\pi(N/V)\int_0^{\infty}\{[(2k_Fr)\cos(2k_Fr)-\sin(2k_Fr)]/(2k_Fr)^4\}r^2dr\ .$$

Introducing $y=2k_Fr$,

$$\begin{aligned}\sum_{\vec{r}}F(2k_Fr)&=4\pi(N/V)(2k_F)^{-3}\int_0^{\infty}[(y\cos y-\sin y)/y^2]dy\\&=4\pi(N/V)(2k_F)^{-3}\int_0^{\infty}\frac{d}{dy}(\sin y/y)dy\\&=-4\pi(N/V)(2k_F)^{-3}\ .\end{aligned} \tag{A6}$$

For $|\vec{k}\cdot\vec{r}|\ll 1$, $e^{i\vec{k}\cdot\vec{r}}$ can be expanded into a power series in $(\vec{k}\cdot\vec{r})$. Retaining only the terms up to $(\vec{k}\cdot\vec{r})^2$, we get

$$\begin{aligned}\sum_{\vec{r}}F(2k_Fr)e^{i\vec{k}\cdot\vec{r}}&=\sum_{\vec{r}}F(2k_Fr)-\pi(N/V)k^2\int_0^{\infty}r^4F(2k_Fr)\left[\int_{-1}^{+1}u^2du\right]dr\\&=\sum_{\vec{r}}F(2k_Fr)-(2\pi/3)(N/V)k^2\int_0^{\infty}\{[(2k_Fr)\cos(2k_Fr)\\&\qquad-\sin(2k_Fr)]/(2k_Fr)^4\}r^4dr\\&=\sum_{\vec{r}}F(2k_Fr)-(2\pi/3)(N/V)k^2(2k_F)^{-5}\int_0^{\infty}(y\cos y-\sin y)dy\\&=\sum_{\vec{r}}F(2k_Fr)+(4\pi/3)(N/V)(2k_F)^{-5}k^2\ .\end{aligned} \tag{A7}$$

The total Hamiltonian can now be written as

$$H=E_0+\sum_{\vec{k}}E(k)b^{\dagger}_{\vec{k}}b_{\vec{k}}$$

with

$$E_0=-g\mu_BH_0NS-NzJS^2-(3AZ/4)S(NS+1)+(3AZ^2/128\pi)NS \tag{A8}$$

and

$$E(k)=g\mu_BH_0+Dk^2\ , \tag{A9}$$

where

$$D=(SAZ/8k_F^2)+SzJa^2/3 \tag{A10}$$

and a is the nearest-neighbor distance. Equations (A8)—(A10) have been obtained in this form by using the relations

$$\sum_{\vec{k}}(\ )=[V/(2\pi)^3]\int d^3k(\ )$$

and $(n/V)=k_F^3/3\pi^2$, where n is the number of electrons, and Eqs. (A6) and (A7). Equation (A9) is nothing but the usual ferromagnetic magnon-dispersion relation with the spin-wave stiffness coefficient D given by Eq. (A10).

Next, we proceed to obtain the expression for the Curie temperature T_C in the molecular-field approximation starting from the Hamiltonian given by Eq. (A1). In the molecular-field approximation, Hamiltonian (A1) can be written in the form

$$H_W=-g\mu_B H_0 N\langle S\rangle - zJN(\langle S\rangle)^2-[J_0 N(\langle S\rangle)^2/2]\sum_{\substack{>\\ n\neq m}} F(2k_F R_{mn})$$

or $(H_W/V)=-H_0 M-(\lambda M^2/2)$, where $M=(N/V)g\mu_B\langle S\rangle$ and

$$\lambda=[2zJ/(N/V)g^2\mu_B^2]+\left[(J_0/(N/V)g^2\mu_B^2)\sum_{\substack{>\\ n\neq m}} F(2k_F R_{mn})\right].$$

With the aid of the well-known molecular-field relation, $T_C=\lambda C$, where $C=[g^2\mu_B^2 S(S+1)/3k_B](N/V)$, and Eq. (A6), we obtain T_C finally in the form

$$T_C=(2/3k_B)S(S+1)[zJ+(3AZ/8)]\ . \tag{A11}$$

From Eqs. (A10) and (A11), D and T_C can be related as follows:

$$D=D_0+mT_C\ , \tag{A12}$$

where

$$D_0=-(SAZ/8)(a^2-k_F^{-2}) \tag{A13}$$

and

$$m=[k_B a^2/2(S+1)]\ . \tag{A14}$$

Using the typical values $a\simeq 2.55$ Å, $k_F\simeq 1.5$ Å^{-1}, $E_F\simeq 10$ eV, $Z=1$, $S=1$, and $J_{sd}(0)=0.1$ eV, we obtain $D_0=-0.76$ meV Å^2.

In order to obtain the maximum value of D_0, we restrict the RKKY interaction to the nearest neighbors only. In this case, the Eqs. (A8), (A10), (A11), and (A13) are modified to

$$E_0'=E_0+(3AZ/4)S(NS+1)[\sin(2k_F a)/(2k_F a)]$$
$$-(3AZ^2/256\pi)NS[(2k_F a)\sin(2k_F a)+2\cos(2k_F a)]\ , \tag{A15}$$

$$D'=D-(SAZ/8k_F^2)[(k_F a)\sin(2k_F a)+\cos(2k_F a)]\ , \tag{A16}$$

$$T_C'=T_C-(AZ/4k_B)S(S+1)[\sin(2k_F a)/(2k_F a)]\ , \tag{A17}$$

$$D_0'=D_0-(SAZ/8)[(a/2k_F)\sin(2k_F a)+\cos(2k_F a)/k_F^2]\ , \tag{A18}$$

where E_0, D, T_C, and D_0 are given, respectively, by Eqs. (A8), (A10), (A11), and (A13). Substituting the values for various parameters as done previously for D_0 in Eq. (A18), we get $D_0'=-0.87$ meV Å^2. Recent resistivity calculations[48] on such amorphous transition-metal–metalloid alloys have shown that for these alloys the more appropriate value for Z is approximately equal to 2. Even with this value of Z, the maximum value for D_0' comes out to be -1.75 meV Å^2. We therefore conclude from the above calculations that the RKKY interaction gives a negative but negligible contribution to the intercept on the ordinate of the D vs T_C curve.

APPENDIX B

We now consider the case when the Heisenberg exchange interaction between localized spins involves not only the nearest neighbors but also the next-nearest neighbors. The Hamiltonian of interest is then

$$H=-g\mu_B H_0\sum_i S_{iz}-\sum_i\sum_{j\neq i} J_{ij}\vec{S}_i\cdot\vec{S}_j\ . \tag{B1}$$

If the spin localized on the site i has z_1 nearest neighbors and z_2 next-nearest neighbors positioned at $\vec{\delta}_1$ and $\vec{\delta}_2$, respectively, relative to i, and if the

corresponding exchange coupling constants are J_1 and J_2, the Hamiltonian (B1) takes the form

$$H=-g\mu_B H_0\sum_i S_{iz}-J_1\sum_i\sum_{\vec{\delta}_1}\vec{S}_i\cdot\vec{S}_{i+\vec{\delta}_1}$$
$$-J_2\sum_i\sum_{\vec{\delta}_2}\vec{S}_i\cdot\vec{S}_{i+\vec{\delta}_2}\,. \tag{B2}$$

Transforming to magnon operators and neglecting the fourth- and higher-order terms as done previously in Appendix A, Eq. (B2) reduces to

$$H=-g\mu_B H_0 NS-(z_1J_1+z_2J_2)NS^2$$
$$+g\mu_B H_0\sum_{\vec{k}}b^\dagger_{\vec{k}}b_{\vec{k}}+2z_1J_1S\sum_{\vec{k}}(1-\gamma^1_{\vec{k}})b^\dagger_{\vec{k}}b_{\vec{k}}$$
$$+2z_2J_2S\sum_{\vec{k}}(1-\gamma^2_{\vec{k}})b^\dagger_{\vec{k}}b_{\vec{k}}\,, \tag{B3}$$

where

$$\gamma^1_{\vec{k}}=z_1^{-1}\sum_{\vec{\delta}_1}\exp(i\vec{k}\cdot\vec{\delta}_1)$$

and

$$\gamma^2_{\vec{k}}=z_2^{-1}\sum_{\vec{\delta}_2}\exp(i\vec{k}\cdot\vec{\delta}_2)\,.$$

In the long-wavelength limit, i.e., $|\vec{k}\cdot\vec{\delta}_1|\ll 1$ and $|\vec{k}\cdot\vec{\delta}_2|\ll 1$, $\gamma^1_{\vec{k}}\cong 1-(a_0k)^2/z_1$, and $\gamma^2_{\vec{k}}\cong 1-(a_0k)^2/z_2$ for cubic lattices of lattice constant a_0, and Eq. (B3) finally simplifies into

$$H=E_0+\sum_{\vec{k}}E(k)b^\dagger_{\vec{k}}b_{\vec{k}} \tag{B4a}$$

with

$$E_0=-g\mu_B H_0 NS-(z_1J_1+z_2J_2)NS^2\,, \tag{B4b}$$

$$E(k)=g\mu_B H_0+Dk^2\,, \tag{B4c}$$

and

$$D=2(J_1+J_2)Sa_0^2\,, \tag{B4d}$$

where D is the spin-wave stiffness coefficient and Eq. (B4c) represents the normal ferromagnetic spin-wave dispersion relation.

For bcc and fcc lattices, Eq. (B4d) can be rewritten as

$$D=(z_1J_1a_1^2+z_2J_2a_2^2)S/3\,, \tag{B5}$$

where a_1 and a_2 denote the nearest- and the next-nearest-neighbor distances, respectively. Note that the first term in Eq. (B5) is also valid for the simple cubic lattice whereas the second term is not.

In order to obtain the expression for the Curie temperature T_C in the molecular-field approximation, we start with the Hamiltonian (B1) and adopt the same procedure as in Appendix A. With the use of the molecular-field approach, the Hamiltonian (B1) can be written in the Weiss form as

$$(H_W/V)=-M[H_0+(\lambda M/2)]$$

with

$$M=\bar{N}g\mu_B\langle S\rangle,\quad \bar{N}=N/V$$

and

$$\lambda=2(z_1J_1+z_2J_2)/\bar{N}g^2\mu_B^2\,.$$

Employing the molecular-field relation

$$T_C=\lambda\bar{N}g^2\mu_B^2S(S+1)/3k_B\,,$$

we obtain T_C as

$$T_C=[2S(S+1)/3k_B](z_1J_1+z_2J_2)\,. \tag{B6}$$

Equations (B5) and (B6) can now be combined to yield the following relation between D and T_C:

$$D=D_0+mT_C\,, \tag{B7}$$

where

$$D_0=z_2J_2(a_2^2-a_1^2)S/3 \tag{B8}$$

and

$$m=k_Ba_1^2/2(S+1)\,. \tag{B9}$$

[1]H. A. Mook, N. Wakabayashi, and D. Pan, Phys. Rev. Lett. 34, 1029 (1975).

[2]J. D. Axe, L. Passel, and C. C. Tsuei, in *Magnetism and Magnetic Materials—1974 (San Francisco)*, Proceedings of the 20th Annual Conference on Magnetism and Magnetic Materials, edited by C. D. Graham, Jr., G. H. Lander, and J. J. Rhyne (AIP, New York, 1975), p. 119.

[3]J. W. Lynn, G. Shirane, R. J. Birgeneau, and H. S. Chen, in *Magnetism and Magnetic Materials—1976 (Joint MMM-Intermag Conference, Pittsburgh)*, Partial Proceedings of the First Joint MMM-Intermag Conference, edited by J. J. Becker and G. H. Lander, (AIP, New York, 1976), p. 313.

[4]J. D. Axe, G. Shirane, T. Mizoguchi, and K. Yamauchi, Phys. Rev. B 15, 2763 (1977).

[5]R. J. Birgeneau, J. A. Tarvin, G. Shirane, E. M. Gyorgy, R. C. Sherwood, H. S. Chen, and C. L. Chien, Phys. Rev. B 18, 2192 (1978).

[6]R. W. Cochrane and G. S. Cargill III, Phys. Rev. Lett. 32, 476 (1974).

[7]C. C. Tsuei and H. Lilienthal, Phys. Rev. B 13, 4899 (1976).

[8]T. Mizoguchi, in *Magnetism and Magnetic Materials—1976,* Ref. 3, p. 286.

[9]N. S. Kazama, M. Mitera, and T. Masumoto, in *Proceedings of the Third International Conference on Rapidly Quenched Metals, Brighton, 1978,* edited by B. Cantor (The Metals Society, London, 1978), p. 164.

[10]S. M. Bhagat, M. L. Spano, and K. V. Rao, J. Appl. Phys. 50, 1580 (1979); S. Hatta and T. Egami, *ibid.* 50, 1589 (1979); R. Hasegawa and R. Ray, Phys. Rev. B 20, 211 (1979).

[11]F. E. Luborsky, J. L. Walter, H. H. Liebermann, and E. P. Wohlfarth, J. Magn. Magn. Mater. 15-18, 1351 (1980).

[12]C. L. Chien and R. Hasegawa, Phys. Rev. B 16, 2115 (1977); 16, 3024 (1977).

[13]C. L. Chien, D. Musser, E. M. Gyorgy, R. C. Sherwood, H. S. Chen, F. E. Luborsky, and J. L. Walter, Phys. Rev. B 20, 283 (1979).

[14]S. Dey, P. Deppe, M. Rosenberg, F. E. Luborsky, and J. L. Walter, J. Appl. Phys. 52, 1805 (1981).

[15]F. Keffer in *Ferromagnetism,* edited by H. P. J. Wijn (Springer, Berlin, 1966), Vol. XVIII, Teil 2, p. 1.

[16]C. Herring and C. Kittel, Phys. Rev. 81, 869 (1951).

[17]T. Kaneyoshi, J. Phys. Soc. Jpn. 45, 1835 (1978); J. Phys. C 5, 3504 (1972).

[18]S. N. Kaul, Phys. Rev. B 24, 6550 (1981), and references quoted therein.

[19]Y. Ishikawa, K. Yamada, K. Tajima, and K. Fukamichi, J. Phys. Soc. Jpn. 50, 1958 (1981).

[20]G. S. Cargill III, in *Magnetism and Magnetic Materials—1974,* Ref. 2, p. 138.

[21]A. Katsuki and E. P. Wohlfarth, Proc. R. Soc. London Ser. A 295, 182 (1966); E. P. Wohlfarth, in *Quantum Theory of Atoms, Molecules, and the Solid State,* edited by P. Löwdin (Academic, New York, 1966), p. 485.

[22]S. N. Kaul, Phys. Rev. B 22, 278 (1980).

[23]S. N. Kaul and M. Rosenberg, Phys. Rev. B 25, 5863 (1982).

[24]B. E. Argyle, S. H. Charap, and E. W. Pugh, Phys. Rev. 132, 2051 (1963).

[25]J. E. Robinson, Phys. Rev. 83, 678 (1951).

[26]R. Hasegawa, in *Magnetism and Magnetic Materials—1975,* Proceedings of the 21st Annual Conference on Magnetism and Magnetic Materials, edited by J. J. Becker, G. H. Lander, and J. J. Rhyne (AIP, New York, 1976), p. 216.

[27]P. E. Tannenwald, J. Phys. Soc. Jpn. Suppl. B1, 17, 592 (1962).

[28]G. S. Cargill III, in *Solid State Physics,* edited by H. Ehrenreich, F. Seitz, and D. Turnbull (Academic, New York, 1975), Vol. 30, p. 227.

[29]At first sight, this linear relation between D and T_C may seem puzzling in view of the finding that D/T_C vs T_C also gives a straight-line curve, but when instead of the latter plot one plots $(D-D_0)/T_C$ against T_C, a straight line parallel to the abscissa results.

[30]G. Hilscher, R. Haferl, H. Kirchmayr, M. Müller, and H. J. Güntherodt, J. Phys. F 11, 2429 (1981).

[31]Y. Yeshurun, K. V. Rao, M. B. Salamon, and H. S. Chen, J. Appl. Phys. 52, 1747 (1981).

[32]J. W. Lynn, R. W. Erwin, J. J. Rhyne, and H. S. Chen, J. Appl. Phys. 52, 1738 (1981).

[33]A. Katsuki, Brit. J. Appl. Phys. 18, 199 (1967).

[34]M. Hatherly, K. Hirakawa, R. D. Lowde, J. F. Mallett, M. W. Stringfellow, and B. H. Torrie, Proc. Phys. Soc. London 84, 55 (1964).

[35]U. Krey, Z. Phys. B 31, 247 (1978).

[36]J. O. Thomson and J. R. Thompson, J. Phys. F 11, 247 (1981); Physica 107B, 635; 107, 637 (1981), J. Appl. Phys. 52, 1782 (1981), and the references quoted therein.

[37]D. G. Onn, T. H. Antoniuk, T. A. Donnelly, W. D. Johnson, T. Egami, J. T. Prater, and J. Durand, J. Appl. Phys. 49, 1730 (1978).

[38]J. Durand, in *Amorphous Magnetism II,* edited by R. A. Levy and R. Hasegawa (Plenum, New York, 1977), p. 305. See also S. J. Poon and J. Durand, *ibid.* p. 245.

[39]S. N. Kaul, Solid State Commun. 36, 279 (1980), and the references cited therein.

[40]M. Sakoh and D. M. Edwards, Phys. Status Solidi B 70, 611 (1975).

[41]D. M. Edwards, J. Magn. Magn. Mater. 15-18, 262 (1980); in *Electron Correlation and Magnetism in Narrow-Band Systems,* edited by T. Moriya (Springer, New York, 1981), p. 73.

[42]Z. Frait, Phys. Status Solidi 2, 1471 (1962).

[43]E. P. Wohlfarth, in *Ferromagnetic Materials,* edited by E. P. Wohlfarth (North-Holland, New York, 1980), Vol. 1, p. 1.

[44]S. N. Kaul, IEEE Trans. Magn. 17, 1208 (1981).

[45]G. S. Grest and S. R. Nagel, Phys. Rev. B 19, 3571 (1979).

[46]R. C. O'Handley, R. Hasegawa, R. Ray, and C. P. Chou, Appl. Phys. Lett. 29, 330 (1976).

[47]C. Kittel, *Quantum Theory of Solids* (Wiley, New York, 1963), p. 50.

[48]E. Esposito, H. Ehrenreich, and C. D. Gelatt, Jr., Phys. Rev. B 18, 3913 (1978).